J Solid State Electrochem (2004) 8: 914–922
DOI 10.1007/s10008-004-0515-z

ORIGINAL PAPER

W. Wang · S. P. Jiang

Effect of polarization on the electrode behavior and microstructure of (La,Sr)MnO_3 electrodes of solid oxide fuel cells

Received: 11 November 2003 / Accepted: 28 January 2004 / Published online: 11 March 2004

Abstract The electrode behavior and microstructure of freshly prepared $(La_{0.8}Sr_{0.2})_{0.9}MnO_3$ (LSM) electrodes were investigated under various polarization conditions. The original, large agglomerates in freshly prepared LSM electrodes were broken down into sphere-shaped grains when exposed to cathodic or anodic current passage of 200 mA cm^{-2} at 800 °C in air for 3 h. Microstructural changes under cathodic polarization could be related to the pronounced diffusion and migration of oxygen vacancies and Mn ions on the LSM surface and lattice expansion, while lattice shrinkage under oxidation conditions most likely contributes to the structural changes under anodic polarization. Such morphological changes were irreversible and were found to be beneficial to the performance of freshly prepared LSM electrodes. Freshly prepared LSM electrodes behaved very differently with respect to the cathodic and anodic current passage treatment.

Keywords (La,Sr)MnO_3 · Solid oxide fuel cells · Polarization treatment · Microstructure · Electrode behavior

Introduction

Sr-doped $LaMnO_3$ (LSM) is the most common cathode material for solid oxide fuel cells due to its high stability and high electrocatalytic activity for O_2 reduction at high temperatures [1, 2, 3]. However, as shown recently [4], there is a complex relationship between the microstructure and electrochemical polarization performance for O_2 reduction on LSM electrodes. The relationship between the microstructure and electrode behavior involves continuous change and evolution under fuel cell operation conditions. A typical example is the initial polarization behavior of LSM electrodes. It has been shown that, for the O_2 reduction reaction on freshly prepared LSM electrodes, the initial polarization losses are very high and decrease significantly with cathodic polarization/current passage [5]. Such an activation effect of cathodic polarization/current passage on the polarization behavior of LSM electrodes has been attributed to the generation of oxygen vacancies [6, 7, 8, 9], the enlargement of the three-phase boundary (TPB) area [10, 11], and the breaking of surface passive layers associated with SrO segregation [12].

In addition to the improvement of polarization performance, cathodic polarization/current passage was found to induce microstructure and morphology changes. Tsukuda et al. [13] studied the effect of cathodic current passage on the electrode properties of $La_{0.9}Sr_{0.1}MnO_3$, and found that microstructure changes occurred at the LSM/YSZ interface after cathodic polarization. This was ascribed to the flux of oxygen vacancies from YSZ electrolyte to the LSM side under cathodic potential. Mizusaki et al. [14], in a study of O_2 reduction on dense LSM films, observed the formation of grains of submicrometer size with clear grain boundaries on originally dense and smooth LSM films after cathodic polarization, an indication of morphological change induced by polarization treatment. Our recent studies show that cathodic polarization causes microstructural change not only at the LSM/YSZ interface but also in the LSM electrode bulk [15]. In this report, we will present additional results of electrode behavior and microstructure observation for LSM electrodes under various current passage/polarization conditions. The results of electrochemical impedance spectroscopy (EIS) and scanning electron microscopy (SEM) indicate that either cathodic or anodic polarization treatment will result in microstructure change at the electrode/electrolyte interface and in the LSM electrode bulk. Such microstructural change has a significant effect on the polarization performance of LSM electrodes.

W. Wang · S. P. Jiang (✉)
Fuel Cell Strategic Research Program, School of Mechanical & Production Engineering, Nanyang Technological University, 50 Nanyang Avenue, 639798 Singapore, Singapore
E-mail: mspjiang@ntu.edu.sg

Experimental

Zirconia electrolyte disks were prepared from 8 mol% Y_2O_3-ZrO_2 (YSZ, Tosoh, Japan) by die-pressing, followed by sintering at 1,500 °C in air for 4 h. The thickness and diameter of sintered YSZ electrolyte disks were ~1 and 18 mm, respectively. A-site nonstoichiometric $(La_{0.8}Sr_{0.2})_{0.9}MnO_3$ (LSM) powders were prepared by coprecipitation and calcined at 900 °C in air. X-ray diffraction (XRD) spectra of the as-fired powder showed the perovskite structure only [16]. LSM electrode ink was applied to the electrolyte substrate by screen-printing and then sintered at 1,150 °C in air for 2 h. The electrode coating thickness was ~15 μm and the electrode coating area was 0.5 cm^2. Pt paste was painted on the other side of the YSZ electrolyte substrate as the counter electrode and reference electrode. The counter electrode was symmetrically positioned at the center, opposite to the working electrode. The reference electrode was painted as a ring around the counter electrode. The gap between counter and reference electrodes was ~4 mm.

All polarization treatments were performed under a current density of 200 mA cm^{-2} at 800 °C in air. The polarization treatments selected in this study were (a) cathodic for 3 h, (b) cathodic and anodic for 6 h, (c) anodic for 3 h, and (d) cathodic, anodic, and cathodic for 9 h. The duration for each individual polarization section was kept as 3 h. The polarization was interrupted from time to time to conduct electrochemical impedance spectroscopy (EIS) measurement using a Solartron 1260 frequency response analyzer in combination with a Solartron 1287 electrochemical interface. The frequency range of EIS was from 0.1 Hz to 100 kHz and the signal amplitude was 10 mV. EIS measurements were performed in a three-electrode arrangement at open circuit. The electrode ohmic resistance (R_Ω) was measured from the high-frequency intercept and the electrode interface (polarization) resistance (R_E) was obtained directly from the difference between the high-frequency and low-frequency intercepts on the impedance curves.

The microstructure of the LSM electrode before and after various polarization treatments was examined by scanning electron microscopy (SEM, Leica S360). At least two samples were tested for each current/polarization treatment to confirm the reproducibility of the microstructure change and electrode behavior. The average particle size of the LSM electrodes after various current passage treatments was directly estimated from SEM pictures taken at different areas of the electrodes.

Results

Polarization behavior

Figure 1 shows the impedance responses and the change of electrode polarization resistance (R_E) of a freshly prepared LSM electrode as a function of cathodic current passage time at 200 mA cm^{-2} and 800 °C in air for 3 h. The absolute value of R_E depended on the individual LSM electrodes. However, the trend of the change of R_E with the cathodic current passage time was the same. R_E shows a very sharp decrease in the first 5 min of cathodic polarization after which the decrease in R_E was much smaller with the current passage time. The initial R_E value was 18.5 Ω cm^2 before cathodic current passage and was reduced significantly to 3.5 Ω cm^2 after 5 min of current passage. At the end of 3 h cathodic polarization treatment R_E was reduced to 0.75 Ω cm^2. This indicates that the activation process of cathodic polarization on the polarization performance of LSM electrodes is rather rapid and is most effective in the first 5 to 15 min of cathodic current passage under present test conditions.

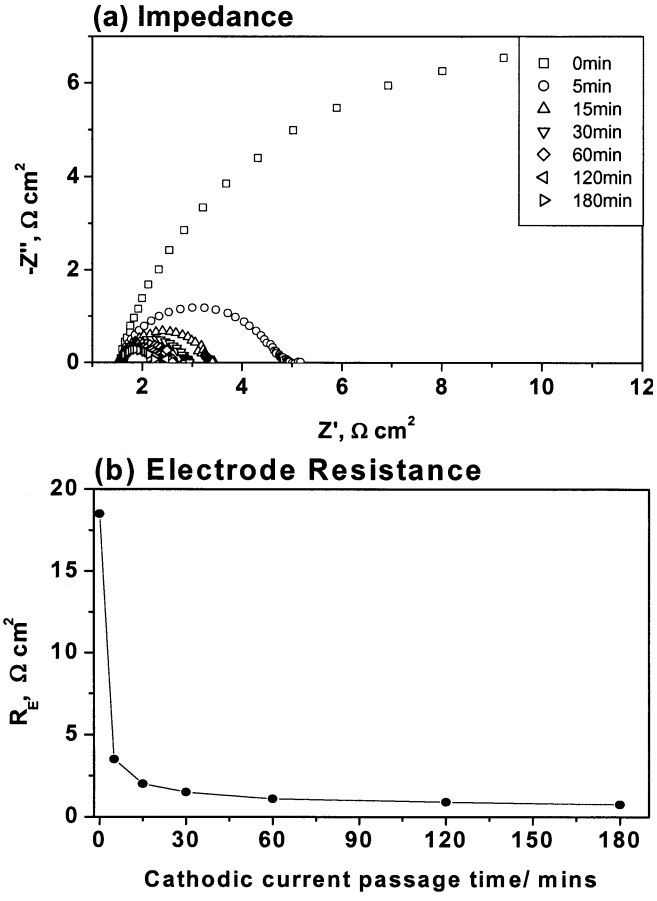

Fig. 1a,b Initial **a** impedance responses and **b** electrode polarization resistances (R_E) of a freshly prepared LSM electrode as a function of cathodic current passage time at 200 mA cm^{-2} and 800 °C in air

Figure 2 shows the impedance responses and electrode polarization resistance of a freshly prepared LSM electrode after 3 h cathodic current passage followed by another 3 h anodic current passage at 200 mA cm^{-2} and 800 °C. Similar to that shown in Fig. 1, a rapid reduction in R_E was observed with cathodic current passage. After the cathodic current passage treatment,

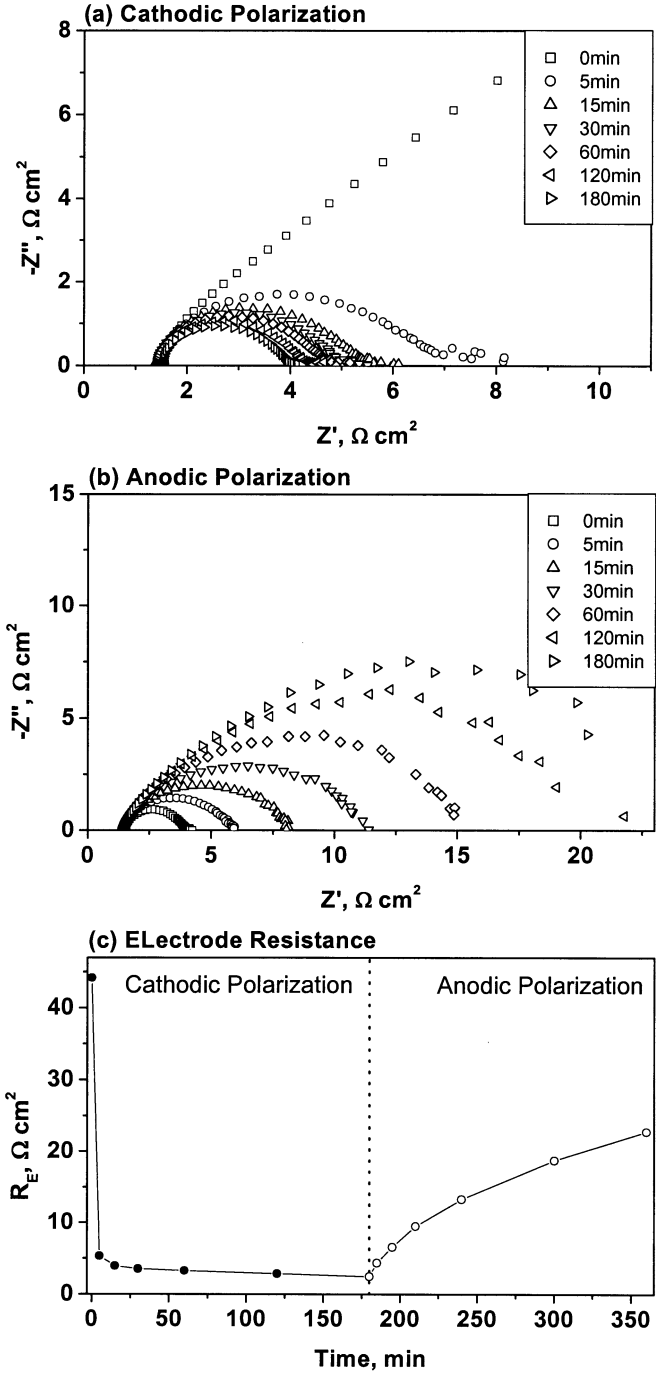

Fig. 2a–c Impedance responses of a freshly prepared LSM electrode with **a** cathodic and then **b** anodic current passage time at 200 mA cm^{-2} and 800 °C in air. The change of electrode polarization resistance (R_E) as a function of different current passage time is shown in **c**

R_E increased with the anodic current passage. However, different from the rapid reduction of R_E with the cathodic current passage, the increase in R_E with anodic current passage time was rather gradual and much slower (Fig. 2c). The increase of R_E with the anodic current passage is an indication of the deactivation effect of anodic polarization on the O_2 reactions on LSM

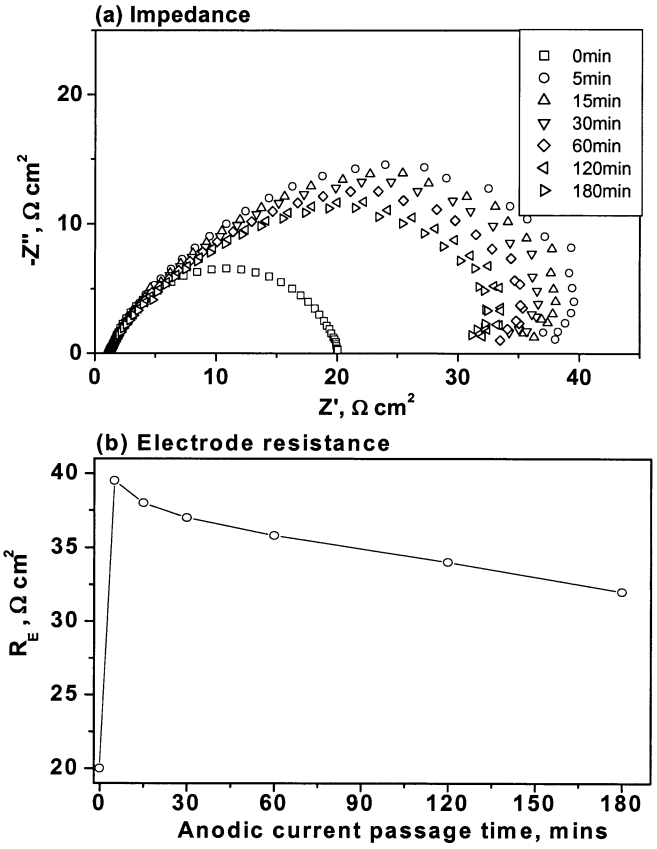

Fig. 3a,b Initial **a** impedance responses and **b** electrode polarization resistances (R_E) of a freshly prepared LSM electrode as a function of anodic current passage time at 200 mA cm^{-2} and 800 °C in air

electrodes. At the end of anodic current passage treatment for 3 h, R_E was 23 Ω cm^2, still smaller than the initial R_E of 43.6 Ω cm^2 before the cathodic current passage. This indicates that the activation effect of cathodic polarization and the deactivation effect of anodic polarization are not reversible in respect of the polarization behavior of LSM electrodes.

The effect of anodic polarization was also studied on a freshly prepared LSM electrode, as shown in Fig. 3. Change of R_E with anodic current passage time can be characterized by two distinct regions: R_E increased very quickly with anodic current passage, followed by a region where R_E showed a gradual decrease (Fig. 3b). R_E was 19 Ω cm^2 before anodic current passage. After 5 min of anodic current passage, R_E increased significantly to 39.5 Ω cm^2. Further anodic current passage treatment led to the monotonous decrease of R_E. After anodic polarization for 3 h, R_E was reduced to 32 Ω cm^2, which was still higher than the initial value of 19 Ω cm^2 before anodic polarization. Such polarization behavior of the freshly prepared LSM electrode with anodic current passage was quite different from that observed on the cathodically polarized LSM electrode (see Fig. 2).

Figure 4 shows the impedance responses and change of electrode polarization resistance as a function of

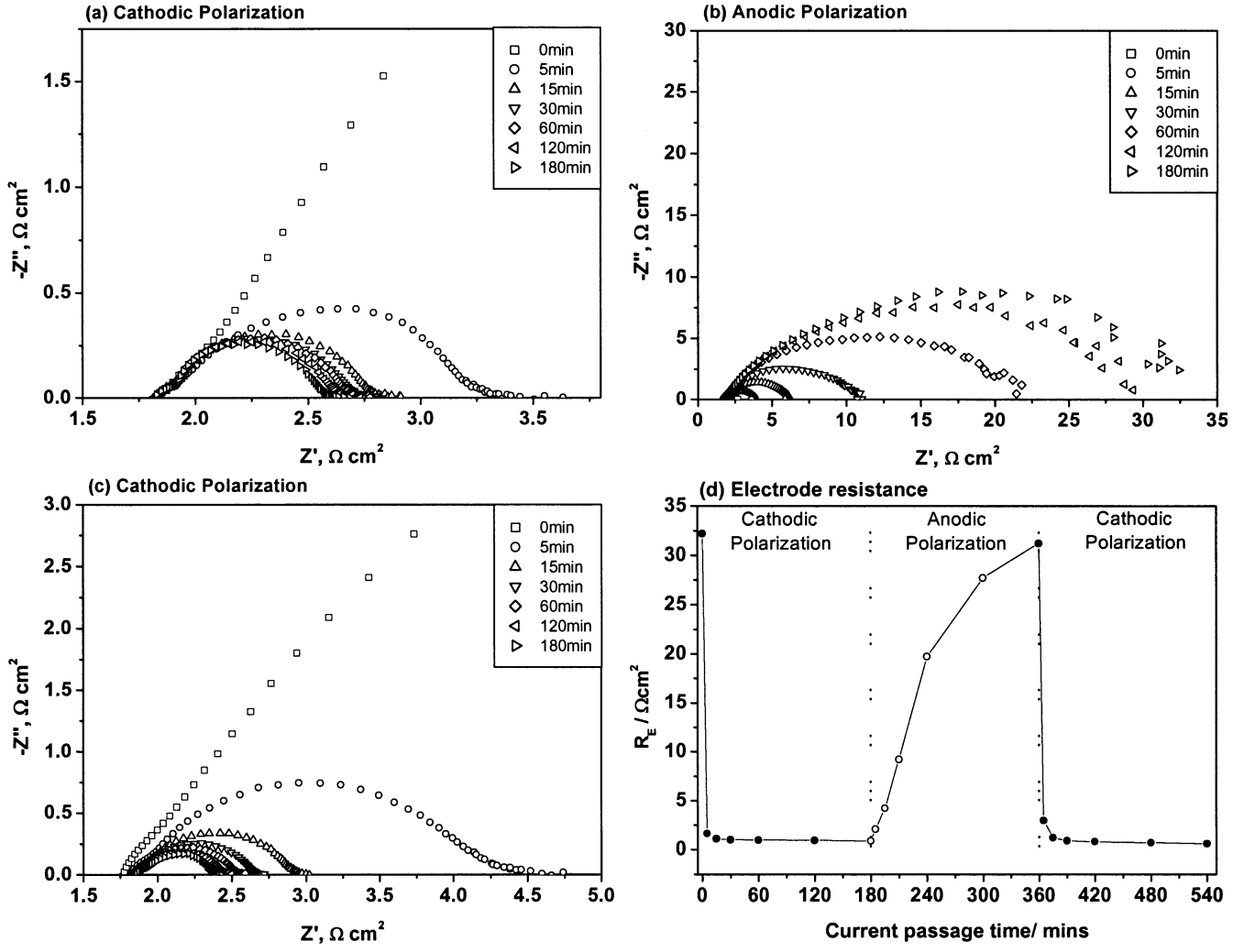

Fig. 4a–d Impedance responses of a freshly prepared LSM electrode with **a** cathodic, **b** anodic, and finally **c** cathodic current passage time at 200 mA cm^{-2} and 800 °C in air. The change of electrode polarization resistance (R_E) as a function of different current passage time is shown in **d**

sequential cathodic, anodic, and then cathodic current passage treatments at 200 mA cm^{-2} and 800 °C in air. The activation effect of cathodic polarization and deactivation effect of anodic polarization were again observed and the rate of increase in R_E with anodic polarization was much smaller than the rate of decrease in R_E with cathodic polarization, similar to that described above (Fig. 2). Moreover, the activation effect of cathodic polarization on anodically polarized LSM electrodes is almost identical to that on freshly prepared LSM electrodes, indicated by the rapid reduction in R_E.

Microstructure observation

Figure 5 shows the SEM pictures of fractured cross sections of LSM electrodes in the bulk and at the electrode/electrolyte interface region before and after cathodic polarization treatment at 200 mA cm^{-2} and 800 °C for 3 h in air. The microstructure of a freshly prepared LSM electrode is characterized by large agglomerates with no clear grain boundaries between LSM particles (Fig. 5a). The bonding between LSM agglomerates and YSZ electrolyte appears to be good, indicated by the continuity between the LSM electrode and YSZ electrolyte phases (Fig. 5c). After cathodic current passage treatment, large agglomerates of the LSM electrode disappeared and the microstructure of the LSM electrode was characterized by much smaller and well-defined granular-shaped particles with clear grain boundaries (Fig. 5b). This is similar to the microstructure change induced by cathodic polarization on LSM electrodes with different composition [15]. However, such change in the microstructure of the LSM electrode does not seem to affect the good bonding between LSM particles and YSZ electrolyte. This is indicated by the continuity at the LSM and YSZ interface (Fig. 5d). There is also a significant increase in small pores due to the microstructural change of the LSM cathode after cathodic current passage.

Figure 6 shows the SEM pictures of freshly prepared LSM electrodes after separate cathodic and anodic current passage for 6 h, anodic current passage for 3 h,

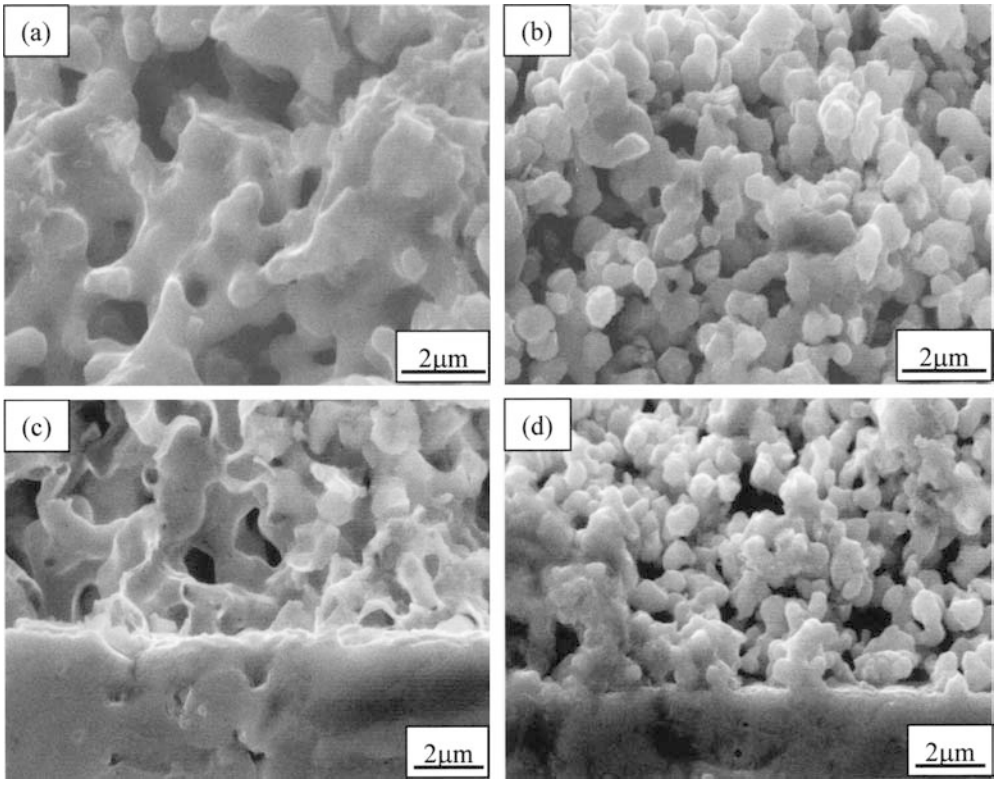

Fig. 5a–d SEM pictures of fractured cross section of a freshly prepared LSM electrode. **a**, **c** Before cathodic current passage; **b**, **d** after cathodic current passage of 200 mA cm^{-2} at 800 °C for 3 h in air. **a** and **b** show the bulk phase and **c** and **d** are the interface region

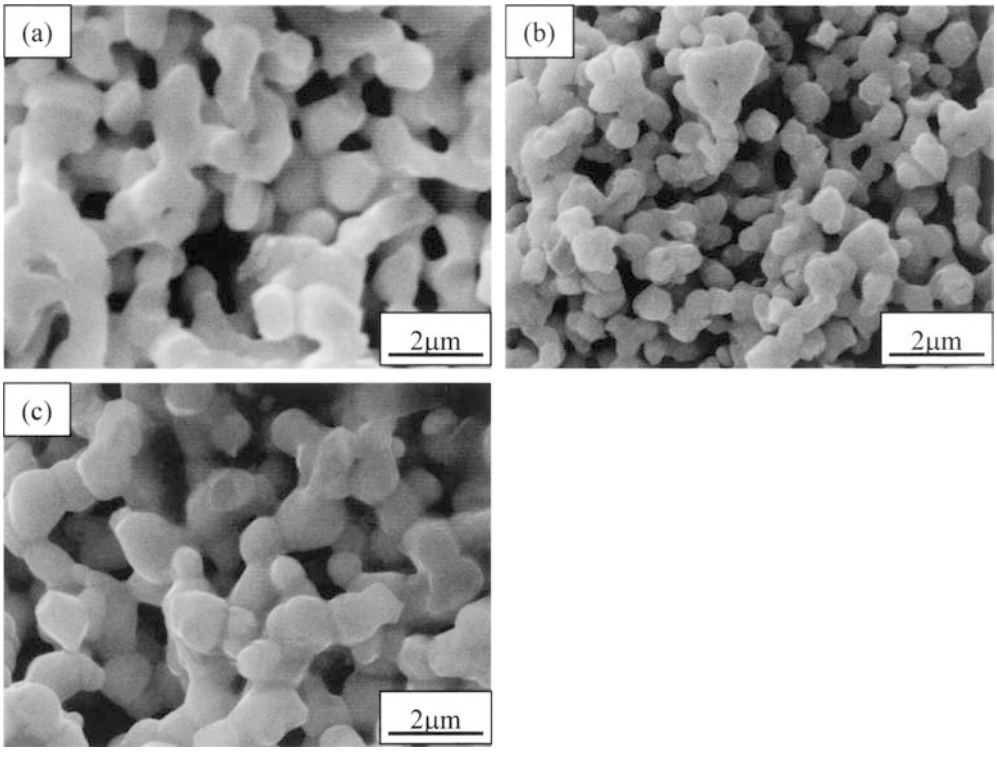

Fig. 6a–c SEM pictures of the fractured cross section of a freshly prepared LSM electrode after **a** cathodic and anodic current passage for 6 h, **b** anodic current passage for 3 h, and **c** cathodic, anodic, and cathodic current passage for 9 h at 200 mA cm^{-2} and 800 °C in air

and cathodic, anodic, and cathodic current passage for 9 h at 200 mA cm^{-2} and 800 °C in air. For the purpose of simplicity, only the SEM pictures of the LSM bulk phase are shown in the figure. However, the microstructural change at the LSM/YSZ interface is similar to that observed in the bulk. Like those after cathodic polarization (see Figs. 5b and 5d), the microstructure of a freshly prepared LSM electrode after cathodic and anodic polarization was characterized by well-defined sphere-shaped particles (Fig. 6a). This indicates that the

morphology change caused by the cathodic current passage treatment cannot be reversed with subsequent anodic current passage treatment. The microstructural change was also observed on a freshly prepared LSM electrode after anodic current passage (Fig. 6b). The morphology change induced by anodic current passage was similar to that after cathodic current passage treatment on a freshly prepared LSM sample (see Fig. 5). This shows that the morphology and microstructure change of the freshly prepared LSM electrode can take place either under cathodic or anodic polarization conditions. Similar morphological change was also observed after sequential cathodic, anodic, and finally cathodic current passage for a total of 9 h (Fig. 6c). However, it appears that LSM particles grow after such sequential polarization treatment. After cathodic current passage for 3 h, the average LSM particle size was estimated to be 0.76 ± 0.18 μm (Fig. 5b). After anodic current passage for 3 h, the average particle size of LSM was 0.67 ± 0.19 μm (Fig. 6b), slightly smaller than that after cathodic current passage treatment. On the other hand, LSM particles grew to 0.89 ± 0.29 μm after cathodic and anodic current passage for 6 h (Fig. 6a) and to 1.04 ± 0.29 μm after cathodic, anodic, and finally cathodic current passage for 9 h (Fig. 6c).

Figure 7 compares the average particle size of LSM electrodes after various current passage treatments. The LSM particles after alternate cathodic, anodic, and cathodic current passage for 9 h was 37% larger than that after cathodic current passage for 3 h. It appears that the increase in the LSM grains is quite significant with alternate cathodic and anodic current passage/polarization.

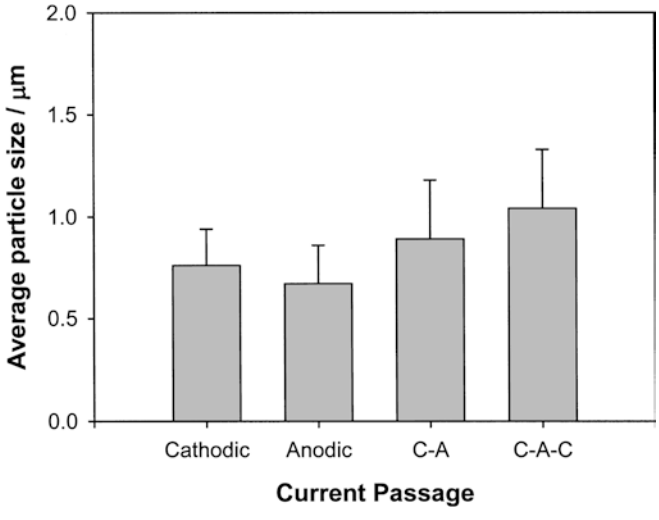

Fig. 7 Average particle size of LSM electrodes after cathodic current passage for 3 h, anodic current passage for 3 h, cathodic and anodic (*C-A*) current passage for 6 h, and cathodic, anodic, and cathodic (*C-A-C*) current passage for 9 h at 200 mA cm^{-2} and 800 °C in air

Discussion

Cathodic current passage/polarization has a significant effect on the polarization behavior of the O_2 reduction reaction on LSM electrodes. As shown in Fig. 1, electrode polarization resistance (R_E) for the reaction on freshly prepared LSM decreased very quickly with the application of cathodic polarization. This is followed by the much slower reduction in R_E with prolonged cathodic polarization, indicating that the activation process of the cathodic current passage treatment is a fast one. The same activation effect of cathodic polarization was also observed on the prior anodically polarized LSM electrodes (see Figs. 2 and 4). An early study on the LSM electrode with and without acid etching treatment indicates that the initial polarization behavior of the freshly prepared LSM electrode could be related to the presence of passivation species such as MnO_x and SrO on the LSM surface [12]. After acid etching treatment of the freshly prepared LSM electrode, the activation effect of cathodic current passage/polarization on the polarization performance of the treated LSM electrode was no longer effective and chemical analysis of the acid solution showed primarily the presence of elemental Mn and Sr. This is consistent with XPS studies of the surface composition of LSM powders, showing strontium enrichment on the LSM surface [17].

Surface segregation of Ca content was also observed on the surface layer of $La_{1-x}Ca_xMnO_3$ powders and their catalytic activity decreased with an increase in the Ca content [18]. The correlation between the catalytic activity of $La_{1-x}Ca_xMnO_3$ perovskites and the surface Ca content was explained by the blocking of the surface active sites by CaO segregated within the surface layer [18]. Similarly, SrO species originally enriched within the surface layer of LSM electrodes can inhibit oxygen surface diffusion by blocking the diffusion path as SrO is an insulator, leading to the initially very high polarization loss of LSM electrodes. Under cathodic polarization conditions and reduced partial pressure of oxygen, SrO on the LSM surface could incorporate into the LSM perovskite phase, eliminating the inhibiting effect of SrO species on the oxygen diffusion process. The incorporation of surface SrO into the LSM perovskite structure could also lead to the formation of oxygen vacancies in the LSM bulk, enhancing the polarization performance of the LSM electrode. Such incorporation of SrO into the A-site of the LSM perovskite structure could be favorable under high temperature and cathodic current passage/polarization (i.e., reducing environment) as the solution energy for the Sr^{2+} substitution of La^{3+} in $LaMnO_3$ perovskites is relatively low [19].

Partial doping of the La^{3+} site in $LaMnO_3$ perovskites with low-valence cations (e.g., Sr^{2+}) will lead to an increase in the valence of the B-site Mn metal ions (as positive holes) and/or the formation of oxygen vacancies. The predominant defect is largely a function of

partial pressure of oxygen [3, 20]. According to the defect model proposed by Mizusaki et al. [21], two defect equilibria can be written as a function of partial pressure of oxygen and temperature:

$$O^{X}_{O,LSM} + 2Mn^{\bullet}_{Mn} \leftrightarrow V^{\bullet\bullet}_{O,LSM} + 2Mn^{\times}_{Mn} + \frac{1}{2}O_2 \quad (1)$$

$$O^{X}_{O,LSM} + 2Mn^{\times}_{Mn} \leftrightarrow V^{\bullet\bullet}_{O,LSM} + 2Mn'_{Mn} + \frac{1}{2}O_2 \quad (2)$$

where $Mn^{\bullet}_{Mn}$, $Mn^{\times}_{Mn}$, and Mn'_{Mn} donate Mn^{4+}, Mn^{3+}, and Mn^{2+} ions, respectively, and $O^{X}_{O,LSM}$ and $V^{\bullet\bullet}_{O,LSM}$ stand for O^{2-} ions and oxygen vacancies in LSM lattice sites. Under fuel cell operation conditions, oxygen vacancies can be generated at the electrode/electrolyte interface region with charge compensation by the reduction of B-site transition metal ions (e.g., Mn^{3+} to Mn^{2+}) according to [8]:

$$O^{X}_{O,LSM} + 2Mn^{3+} + V^{\bullet\bullet}_{O,YSZ} + 2e \rightarrow V^{\bullet\bullet}_{O,LSM} + 2Mn^{2+} + O^{X}_{O,YSZ} \quad (3)$$

where $O^{X}_{O,YSZ}$ and $V^{\bullet\bullet}_{O,YSZ}$ are the O^{2-} ions and oxygen vacancies in YSZ lattice sites, respectively. This shows that oxygen vacancies are not only generated at the electrode/electrolyte interface region but also in the bulk regions of the electrode as a result of the reduced partial pressure of oxygen under cathodic current passage/polarization. Oxygen vacancies formed at the LSM/YSZ interface region would propagate, extending the reactive sites for the O_2 reduction reaction [8]. The electrochemical improvement in activity is thus believed to result from the favorable broadening of the active reaction zone as a result of the formation of oxygen vacancies [6, 7].

The polarization behavior of freshly prepared LSM electrodes under anodic current passage is very different from that under cathodic current passage. For a freshly prepared LSM electrode, a very sharp increase of electrode polarization resistance (R_E) was observed after applying anodic polarization for 5 min and this was followed by a gradual decrease in R_E with anodic current passage time (Fig. 3). Nevertheless, after anodic current passage for 3 h, the R_E was still higher than the initial value for the freshly prepared LSM electrode before the current passage treatment. However, in the case of cathodically polarized LSM electrodes, R_E increased with the anodic current passage time (Figs. 2 and 4), which is consistent with the results observed by Yamashita and Tsukuda [22].

There may exist two possible effects of anodic current passage on the electrode behavior of freshly prepared LSM electrodes. Under anodic polarization conditions, LSM is in the oxidation environment and would exhibit apparent oxygen excess nonstoichiometry. According to the defect model (Eqs. 1 and 2) [21], charge compensation for the excess oxygen would be met by the oxidation of the B-site Mn ions with the concomitant decrease of oxygen vacancies. The reduction in oxygen vacancies could lead to the increase in polarization resistance for the oxygen oxidation (evolution) reaction, as LSM is predominantly an electronic conductor with little ionic conductivity [23]. O_2 could only be evolved at the three-phase boundary (TPB) region. A decrease in oxygen vacancies could also cause SrO segregation from the perovskite structure to the LSM surface layers, again leading to the increase in the electrode polarization resistance for the reaction. On the other hand, the microstructure and morphology of the LSM electrode also change under anodic current passage, similar to those observed under cathodic current passage (Fig. 6b). The transition from large agglomerates to sphere-shaped particles increases the three-phase boundary area between gas, LSM electrode, and YSZ electrolyte, resulting in the reduction of the polarization resistance for the O_2 oxidation reaction. The subsequent decrease in R_E with the anodic current passage time (Fig. 3b) indicates that the positive effect of morphology improvement became predominant, compensating the negative effect of the decrease in the oxygen vacancies in the LSM electrodes. As the morphological change induced either by cathodic current passage or by anodic current passage is not reversible (see Fig. 6), the beneficial effect of the morphology improvement induced by anodic polarization for the O_2 oxidation reaction on prior cathodically polarized LSM electrodes is therefore no longer operative. Thus, the polarization resistance would increase with the increase of anodic current passage time due to the continuous decrease in oxygen vacancies until the pressure of O_2 generated at the interface is high enough to cause delamination at the electrode/electrolyte interface [22]. The very fast initial increase of R_E for the reaction on the freshly prepared LSM electrode as compared to that on the prior cathodically polarized LSM electrode could be the magnified effect of the reduction in oxygen vacancies on originally large and plate-like agglomerates with very low three-phase boundary areas.

It should be pointed out here that delamination at the LSM electrode/YSZ electrolyte interface may not occur in the present studies. This is indicated by the very stable electrode ohmic resistance before and after various current passage treatments. SEM examination of LSM electrodes at the electrode/electrolyte interface region after 3 h of anodic polarization showed no evidence for delamination. However, after anodic current treatment at 200 mA cm^{-2} and 800 °C for more than 25 h, the LSM electrode coating was observed to be completely delaminated from the YSZ electrolyte. Yamashita et al. [22] studied the effect of cathodic and anodic polarization on the electrode performance of $La_{0.9}Sr_{0.1}MnO_3$, and found that the LSM electrode adhered well to the YSZ electrolyte after anodic current treatment at 300 mA cm^{-2} for 5 h but delaminated after ~10 h of anodic current treatment. The delamination is most likely caused by the high oxygen pressure generated at the electrode/electrolyte interface due to the O_2 oxidation reaction.

As shown by the SEM studies of freshly prepared LSM electrodes (Figs. 5 and 6), the change in microstructure and morphology can be induced by either cathodic or anodic current passage. The microstructure change of LSM electrodes under polarization is clearly irreversible, as shown by the stability of the sphere-like morphology of LSM electrodes after repetitive current passage treatments (Fig. 6). The microstructure changes induced by cathodic current passage could be explained by the generation and migration of oxygen vacancies and Mn ions under cathodic polarization conditions. As shown recently by Miyoshi et al. [24], the lattice of LSM perovskites expanded in a reduction environment at low partial pressure of oxygen. This is due to the fact that when oxygen vacancies are introduced (i.e., an increase of oxygen nonstoichiometry) due to reduced partial pressure of oxygen, the charge neutrality in the LSM structure would be maintained by the reduction of transition metal ions in the LSM B-site to the lower valence state (Eqs. 1 and 2), leading to an increase of the averaged ionic radius of the cation and thus lattice expansion. The effect of an increase in B-site radius could be partially offset by the increase in the crystallographic distortion [24].

Lattice expansion upon reduction has also been studied on $LaCrO_3$-based interconnect materials [25, 26]. Similar to the effects in a reducing environment at low partial pressure of oxygen, lattice expansion and crystallographic distortion of the LSM perovskite structure could also occur under cathodic current passage/polarization conditions. It is known that manganese species such as Mn^{3+} and Mn^{2+} ions are also mobile under fuel cell operating conditions, as shown by the extensive Cr deposition on the YSZ electrolyte surface which has been shown to be initiated by the Mn^{2+} ions migrated from LSM electrodes [27, 28]. Weber et al. [29] studied the microstructure change of $La_{0.8}Sr_{0.2}MnO_3$ cathodes operated at 950 °C for ~2,000 h and observed the migration of Mn out of the cathode and into the zirconia electrolyte, in addition to the significant grain growth and densification. Lattice expansion, crystallographic distortion, and cation migration could all weaken the contacts between particles of the agglomerates, leading to the disintegration of the agglomerating structure into sphere-shaped particles. Diffusion of oxygen vacancies generated under cathodic polarization is most likely through diffusion on the LSM surface [23, 30]. Therefore, morphological change from an agglomerating structure to sphere-shaped particles induced by cathodic polarization would promote the O_2 reduction reaction, as the surface diffusion path of oxygen would be shorter on sphere-shaped particles as compared to that on larger agglomerates. However, morphological change induced by prolonged cathodic polarization can cause pore formation and increase the porosity of LSM electrodes, leading to performance degradation [31]. On the other hand, prolonged sintering at 1,000 °C under open circuit conditions in air has little effect on the microstructure and performance of LSM electrodes [31].

Similar to the observations under cathodic current passage, large agglomerates in freshly prepared LSM electrodes changed to sphere-like particles with clear grain boundaries after anodic current passage treatment at 200 mA cm^{-2} and 800 °C for 3 h (Fig. 6b). According to the defect model (Eqs. 1 and 2) [21], $LaMnO_{3-\delta}$ displays not only oxygen-deficit but also oxygen-excess nonstoichiometry. Under anodic current passage/polarization or oxidation conditions, LSM perovskites could incorporate excess oxygen with the valence increase of the transition metal ions in the LSM B-site and/or the creation of cation vacancies, leading to lattice shrinkage similar to that observed on $LaMnO_{3-\delta}$ [32, 33]. Thus, the morphology and microstructure change of freshly prepared LSM electrodes under anodic current passage/polarization is most likely related to the shrinkage of unit cells of LSM in an oxidation environment. This appears to be supported by the slightly smaller grain size of the LSM electrode after anodic current passage at 200 mA cm^{-2} and 800 °C for 3 h (0.67 ± 0.19 μm) as compared to that (0.76 ± 0.18 μm) after cathodic current passage under the same conditions. LSM lattice expansion and shrinkage under cathodic and anodic polarization could be the reason for the observed relatively fast grain growth of LSM electrodes after alternate cathodic and anodic current passage treatment (Fig. 7). The irreversibility in the microstructure and morphology change under cathodic or anodic current passage explains the partial irreversibility of the initial LSM polarization behavior observed on the freshly prepared LSM electrodes [5, 8].

Conclusions

The effect of polarization has been studied on freshly prepared LSM electrodes at 800 °C in air under different polarization conditions. Cathodic current passage/polarization was found not only to enhance the polarization performance of LSM electrodes, but also to improve their microstructure and morphology. The generation and migration of oxygen vacancies and Mn ions, and lattice expansion and crystallographic distortion under cathodic current passage could all contribute to the microstructural changes. Similar to the observations under cathodic current passage, anodic current passage also induced microstructure and morphology improvement in freshly prepared LSM electrodes, which is most likely due to lattice shrinkage in an oxidation environment.

The performance of freshly prepared LSM electrodes for O_2 reduction reactions is improved significantly under cathodic current passage/polarization. In addition to the microstructure enhancement, cathodic polarization could reduce the content of passivation species such as SrO on the LSM surface layers [12] and promote the generation of oxygen vacancies [8], leading to the broadening of the three-phase boundary areas for the O_2 reduction. In the case of freshly prepared LSM elec-

trodes, anodic polarization would lead to a decrease of oxygen vacancies due to the increased oxygen excess nonstoichiometry under oxidation conditions and at the same time enhance the microstructure of the LSM electrode. The microstructure change from large agglomerate to sphere-like particles with clear grain boundaries increases the three-phase boundary regions for the O_2 oxidation reaction. This explains the observed initial increase and then gradual decrease in R_E of the freshly prepared LSM electrode with anodic current passage time.

Acknowledgement W. Wang thanks the Nanyang Technological University for the graduate research studentship.

References

1. Badwal SPS (2001) Solid State Ionics 143:39
2. Mitterdorfer A, Gauckler LJ (1998) Solid State Ionics 111:185
3. Mizusaki J, Yonemura Y, Kamata H, Ohyama K, Mori N, Takai H, Tagawa H, Dokiya M, Naraya K, Sasamoto T, Inaba H, Hashimoto T (2000) Solid State Ionics 132:167
4. Jiang SP (2003) J Power Sources 124:390
5. Jiang SP, Love JG, Zhang JP, Hoang M, Ramprakash Y, Hughes AE, Badwal SPS (1999) Solid State Ionics 121:1
6. Hammouche A, Siebert E, Hammou A, Kleitz M, Caneiro A (1991) J Electrochem Soc 138:1212
7. Siebert E (1994) Electrochim Acta 39:1621
8. Lee HY, Cho WS, Oh SM, Wiemhöfer H–D, Göpel W (1995) J Electrochem Soc 142:2659
9. Jiang Y, Wang S, Zhang Y, Yan J, Li W (1998) J Electrochem Soc 145:373
10. Mizusaki J, Tagawa H, Tsuneyoshi K, Sawata A (1991) J Electrochem Soc 138:1867
11. Odgaard M, Skou E (1996) Solid State Ionics 86–88:1217
12. Jiang SP, Love JG (2001) Solid State Ionics 138:183
13. Tsukuda H, Yamashita A (1994) In: Bossel U (ed) Proceedings of the 1st European solid oxide fuel cells forum, Lucerne, 3–7 October 1994, pp 715–724
14. Mizusaki J, Saito T, Tagawa H (1996) J Electrochem Soc 143:3065
15. Jiang SP, Love JG (2003) Solid State Ionics 158:45
16. Jiang SP, Zhang JP, Ramprakash Y, Milosevic D, Wilshier K (2000) J Mater Sci 35:2735
17. Decorse P, Caboche G, Dufour L-C (1999) Solid State Ionics 117:161
18. Isupova LA, Tsybulya SV, Kryukova GN, Alikina GM, Boldyreva NN, Yakovleva IS, Ivanov VP, Sadykov VA (2001) Solid State Ionics 141–142:417
19. Islam MS, Cherry M, Winch LJ (1996) J Chem Soc Faraday Trans 92:479
20. Van Roosmalen JAM, Cordfunke EHP, Helmhodt RB (1994) J Solid State Chem 110:100
21. Mizusaki J, Mori N, Takai H, Yonemura Y, Minamiue H, Tagawa H, Dokiya M, Inaba H, Naraya K, Sasamoto T, Hashimoto T (2000) Solid State Ionics 129:163
22. Yamashita A, Tsukuda H, Hashimoto T (1994) In: Bossel U (ed) Proceedings of the 1st European solid oxide fuel cells forum, Lucerne, 3–7 October 1994, pp 661–669
23. Carter S, Selcuk A, Chater RJ, Kajda J, Kilner A, Steele BCH (1992) Solid State Ionics 53–56:597
24. Miyoshi S, Hong J-O, Yashiro K, Kaimai A, Nigara Y, Kawamura K, Kawada T, Mizusaki J (2003) Solid State Ionics 161:209
25. Zuev A, Singheiser L, Hilpert K (2000) Solid State Ionics 147:1
26. Mori M, Hiei Y, Yamamoto T (2001) J Am Ceram Soc 84:781
27. Jiang SP, Zhang JP, Foger K (2001) J Electrochem Soc 148:C447
28. Jiang SP, Zhang JP, Apateanu L, Foger K (2000) J Electrochem Soc 147:4013
29. Weber A, Männer R, Jobst B, Schiele M, Cerva H, Waser R, Ivers-Tiffée E (1996) In: Poulsen FW, Bonanos N, Linderoth S, Mogensen M, Zachau-Christiansen B (eds) Proceedings of the 17th Risø international symposium on materials in scientific high temperature electrochemistry: ceramics and metals, Risø National Laboratory, Roskilde, 1996, p 473
30. Jiang SP (2001) J Appl Electrochem 31:181
31. Jorgensen MJ, Holtappels P, Appel CC (2000) J Appl Electrochem 30:411
32. Töpfer J, Goodenough JB (1997) J Solid State Chem 130:117
33. Hauback BC, Fjellvag H, Sakai N (1996) J Solid State Chem 124:43